Published in final edited form as:

Hum Genet. 2007 January ; 120(5): 653–662. doi:10.1007/s00439-006-0246-6.

A new locus for autosomal dominant amelogenesis imperfecta on chromosome 8q24.3

Gustavo Mendoza and **Trevor J. Pemberton**

Institute for Genetic Medicine, University of Southern California, 2250 Alcazar Street, CSC-240, Los Angeles, CA 90033, USA pragna@usc.edu

Kwanghyuk Lee

Department of Molecular and Human Genetics, Baylor College of Medicine, Houston, TX, USA

Raquel Scarel-Caminaga

School of Dentistry, University of São Paulo State, UNESP, Araraquara, Sao Paulo, Brazil

Ruty Mehrian-Shai and **Catalina Gonzalez-Quevedo**

Institute for Genetic Medicine, University of Southern California, 2250 Alcazar Street, CSC-240, Los Angeles, CA 90033, USA pragna@usc.edu

Vasiliki Ninis

Department of Neurology, Baylor College of Medicine, Houston, TX, USA

Jaana Hartiala and **Hooman Allayee**

Institute for Genetic Medicine, University of Southern California, 2250 Alcazar Street, CSC-240, Los Angeles, CA 90033, USA pragna@usc.edu

Malcolm L. Snead

Center for Craniofacial Molecular Biology, University of Southern California, Los Angeles, CA, USA

Suzanne M. Leal

Department of Molecular and Human Genetics, Baylor College of Medicine, Houston, TX, USA

Sergio R. P. Line

Faculty of Odontology of Piracicaba, UNICAMP, Campinas, Sao Paulo, Brazil

Pragna I. Patel

Institute for Genetic Medicine, University of Southern California, 2250 Alcazar Street, CSC-240, Los Angeles, CA 90033, USA pragna@usc.edu

Center for Craniofacial Molecular Biology, University of Southern California, Los Angeles, CA, USA

Abstract

Amelogenesis imperfecta (AI) is a collective term used to describe phenotypically diverse forms of defective tooth enamel development. AI has been reported to exhibit a variety of inheritance patterns, and several loci have been identified that are associated with AI. We have performed a genome-wide scan in a large Brazilian family segregating an autosomal dominant form of AI and mapped a novel locus to 8q24.3. A maximum multipoint LOD score of 7.5 was obtained at marker

D8S2334 (146,101,309 bp). The disease locus lies in a 1.9 cM (2.1 Mb) region according to the Rutgers Combined Linkage-Physical map, between a VNTR marker (at 143,988,705 bp) and the telomere (146,274,826 bp). Ten candidate genes were identified based on gene ontology and microarray-facilitated gene selection using the expression of murine orthologues in dental tissue, and examined for the presence of a mutation. However, no causative mutation was identified.

Introduction

Enamel is formed by the mineralization of an extracellular matrix that contains proteins secreted primarily by ameloblasts (Paine et al. 2001). Amelogenesis imperfecta (AI) is both a clinically and genetically heterogeneous group of disorders affecting tooth enamel formation. AI is primarily characterized by its mode of inheritance (i.e. autosomal dominant or recessive) and secondarily by the enamel phenotype (i.e. hypoplastic or hypomineralised) (Aldred et al. 2003). The prevalence of AI varies between populations. It is relatively common in Sweden where 1 in 700 are affected. It is less common in the USA and Israel, where 1 in 14,000 and 1 in 8,000 are affected, respectively (Witkop 1976; Chosack et al. 1979; Sundell 1986; Backman and Holm 1986; Dong et al. 2000). AI patients display poor aesthetics and dental sensitivity that often requires extensive dental treatment, and the disease has a marked impact on the psychosocial health of affected people comparable with the impact of systemic health conditions, especially at younger ages (CoYeld KD et al. 2005).

Five genes have been previously associated with various forms of AI: *AMELX*, *KLK4*, *MMP20*, *DLX3*, and *ENAM*. Mouse models have identified two additional genes, ameloblastin (*AMBN*; 4q21) (Paine et al. 2003) and tuftelin (*TUFT1*; 1q21) (Luo et al. 2004) that cause phenotypes with enamel defects, when the gene is knocked-out or over-expressed, respectively. Ameloblastin-null mice develop severe enamel hypoplasia caused by the dental epithelium differentiating into the enamel-secreting ameloblasts that are incapable of attaching to the matrix. In a mouse model overexpressing tuftelin, gross imperfections are observed in the enamel with an apparent loss of restricted enamel crystallite growth along their *a*-axis and *b*-axis that results in a change in the crystallite aspect-ratio.

X-linked AI has been associated with the amelogenin (*AMELX*) locus on Xp22.3 (Lagerstrom et al. 1991). Mutational analyses have identified 14 different *AMELX* mutations in kindreds afflicted with this type of AI (reviewed in Stephanopoulos et al. 2005). Amelogenin constitutes ~90% of the total organic enamel matrix protein (Wright et al. 1997), and it is reported to be important for the maintenance of enamel structure and appositional crystal growth during the early to mid-secretory stage of enamel formation (Bartlett et al. 2006).

Autosomal recessive AI has been associated with mutations in the genes encoding kallikrein 4 (*KLK4*) at 19q13.4 (Hart et al. 2004), matrix metalloproteinase 20 (*MMP20*) at 11q22.3-q23 (Ozdemir et al. 2005) and enamelin (*ENAM*) at 4q21 (Hart et al. 2003). KLK4 and MMP20 are enamel-specific proteases that have only recently been characterized. MMP20 has shown expression restricted to the ameloblasts and odontoblasts of developing teeth

(Bartlett et al. 1996; Caterina et al. 1999) where it is reported to be involved in the organization and mineralization of the enamel matrix in the mantle dentin and the efficient reabsorption of enamel matrix proteins (Bartlett et al. 2006; Beniash et al. 2006). KLK4 has been reported to be essential for the final crystallite growth of enamel, but not for the orientation, prism formation, or thickness of this growth (Wright et al. 2006). Both MMP20 and KLK4 have been found to degrade enamel matrix proteins early in the maturation stages (Espiritu-Santo and Line 2005). ENAM represents between 1 and 5% of total enamel matrix protein (Wright et al. 1997), with proteolytic processing giving rise to multiple enamelin cleavage products that localize to different parts of the developing enamel (Hu et al. 1997), suggesting that the different isoforms have varying functions within enamel mineralization.

Autosomal dominant AI (ADAI) has been associated with mutations in the enamelin gene (Rajpar et al. 2001), and in the distal-less homeobox 3 (*DLX3*) gene at 17q21. (Price et al. 1999) The latter is a member of the DLX family of proteins that share similar DNA-binding sites and are thought to act as homeodomain transcription factors in a variety of developmental processes that include osteogenesis, which is considered critical for craniofacial and tooth development (Dong et al. 2005). We report here the identification of a novel locus for ADAI on the long arm of chromosome 8 at 8q24.3 by conventional linkage analysis. Candidate genes were identified based on gene ontology and microarray-facilitated gene selection using the expression of murine orthologues in dental tissue, and examined for the presence of a mutation.

Methods

Family information

A Brazilian family with a hypomineralised autosomal dominant form of amelogenesis imperfecta (Fig. 1) was the subject of this study. The enamel was softer than normal with a creamy yellow to white appearance. The enamel was easily abraded leaving an irregular surface (Fig. 2). Both the deciduous and permanent dentition was affected. There were no differences in the aspects of affected enamel between male and female subjects. This study was carried out with the approval of the FOP/UNICAMP Ethics Committee (protocol 217/04) and informed consent was obtained from all subjects.

Extraction of genomic DNA and genotyping

Venous blood samples were obtained from 35 family members including 18 affected individuals. Genomic DNA was extracted from whole blood using the Gentra Puregene system (Minneapolis, MN) following their standard protocol. A genome-scan was carried out on 27 DNA samples at the Center for Inherited Disease Research at Johns Hopkins University. A total of 410 short tandem repeat polymorphism markers with an average heterozygosity of 0.75 were genotyped. These markers are spaced approximately 10 cM apart and are located on the 22 autosomes and the X and Y chromosomes. After the completion of the genome-scan, DNA from Five additional family members and samples from 26 family members that were included in the genome-scan were used for Fine-mapping the ADAI locus.

For Fine-mapping, polymerase chain reactions (PCR) for microsatellite markers were performed in a total volume of 15 μl with 10 ng of genomic DNA, 0.84 mM of each primer, 266 μM of dNTPs, 1.5 mM of $MgCl_2$, 1 U *Taq* DNA polymerase and 1 × PCR buffer (Invitrogen Life Technologies, Carlsbad, CA. USA). PCR was carried out for 35 cycles: 95°C 1 min, 60°C 1 min and 72°C for 1 min in a Biometra T-Gradient thermocycler (Biometra, Goettingen, Germany). PCR products for six markers were resolved on 6% denaturing acrylamide-polyacrylamide gel using terminal^{32}P-labeling and genotypes were assigned by visual inspection. The other Five markers were Xuorescently labeled with 6-FAM and analyzed on an ABI-3100 genetic analyzer (Applied Biosystems, Foster City, CA, USA).

Linkage analysis

The National Center for Biotechnology Information (NCBI) Build 35 sequence-based physical map was used to determine the order of the genome-scan markers and Fine-mapping markers (Table 1; International Human Genome Sequence Consortium). Several of the Fine-mapping markers were not found on the NCBI sequence-based physical map and were placed on the sequence-based physical map using e-PCR (Schuler 1997). Genetic map distances according to the Rutgers combined linkage-physical map of the human genome were used to carry out the multipoint linkage analysis for the Fine-map and genome-scan markers (Kong et al. 2004). For those Fine-mapping markers for which no genetic map position was available, interpolation was used to place these markers on the Rutgers combined linkage-physical map. PEDCHECK (O'Connell and Weeks 1998) was used to identify Mendelian inconsistencies. Two-point linkage analysis was carried out using the MLINK program of the FASTLINK computer package for the genome-scan and Fine-mapping marker loci (Cottingham et al. 1993). Multipoint linkage analysis was performed using LINKMAP of the FASTLINK computer package (Cottingham et al. 1993) and SIMWALK2 (Sobel and Lange 1996). All markers in the region of interest on chromosome 8 were analyzed simultaneously using SIMWALK2. For the LINKMAP program, the number of markers which could be analyzed together is limited. Therefore, a sliding window containing 2–4 markers was used to carry out the analysis. Although it is possible to perform multipoint analysis with all the marker loci using SIM-WALK2, a disadvantage is that it only provides approximate LOD scores, while LINKMAP is limited in the number of marker loci which can be analyzed but it does report exact LOD scores. For both two-point and multipoint analyses, an autosomal dominant mode of inheritance with complete penetrance and a disease allele frequency of 0.001 was used. For genome-scan markers, the allele frequencies were estimated from the founders and reconstructed founders from this pedigree (Fig. 1) and two additional Brazilian pedigrees that underwent a genome-scan at the same time. For the Fine-mapping markers, equal allele frequencies were used. Haplotypes were constructed using SIMWALK2 (Sobel and Lange 1996)

DNA sequencing

Primers covering the exons of *EPPK1*, *LOC392275*, *GRINA*, *SLC39A4*, *GPAA1*, *COMMD5*, *VPS28*, *FOXH1*, *ZNF34* and *ZNF517* genes were designed using Primer3 version 0.2 (Massachusetts Institute of Technology, Boston, MA). PCR amplification using these primers (available upon request) was optimized for standard dye-terminator

sequencing using the Big-Dye Terminator 3.1 fluorescent sequencing technology on an ABI3100 genetic analyzer (Applied Biosystems, Foster City, CA). DNA sequencing results were analyzed using Sequencing Analysis version 3.7 (Applied Biosystems, Foster City, CA).

Microarray analysis of gene expression in mouse dental tissue

Molar teeth were manually extracted from 60 mouse pups between 1 and 10 days post-natal (USC IACUC Protocol # 7225). The teeth were ground in the presence of liquid nitrogen using a pestle and mortar and the RNA extracted using the RNeasy RNA purification kit (Qiagen, Valencia, CA, USA) following the manufacturer's recommended protocol. The RNA was hybridized to the Affymetrix Mouse Genome Expression 430 2.0 microarrays following the manufacturer's recommended protocols. Microarrays hybridized with mouse dental RNA were analyzed in quadruplicate and compared to a control set of 16 tissues (NCBI GEO database (Edgar et al. 2002); Accession number GSE1986) using the Bioconductor open-source analysis program run within the R-script environment (Gentleman et al. 2004) and the *limma* package (Smyth 2004) to identify genes within our region that exhibited differential expression between the dental and control tissues. Briefly, raw microarray data was normalized using the log-additive robust-multichip-average (RMA) algorithm (Irizarry et al. 2003). The data from the four dental microarray replicates was compared to that of the 16 control tissues by fitting a linear model to the expression data for each probe. The resulting coefficients for each probe were then subjected to a pair-wise comparison between the "dental" versus "control" data and differential expression identified by calculating moderated *t* statistics and log-odds of differential expression by empirical Bayes shrinkage of the gene-wise sample variances towards a common value (Smyth 2004).

Results

Affected individuals were identified in all generations of family AMI1 and both deciduous and permanent dentitions were affected. There were no differences in the aspects of affected enamel between male and female subjects and in teeth from deciduous and permanent dentitions. Observation of altered enamel was possible in only five individuals (V:2, V:3, V:8, V:11, V:12), and in one third molar extracted by surgical indication (IV:5). In the other affected individuals, all teeth had been restored with full crowns or extracted. In most cases, affected incisors and canines presented sharp and irregular edges, that occurred due to total abrasion of enamel layer. Posterior teeth were short due to loss of enamel on the occlusal surfaces and abrasion of underlying dentin. Observation of affected enamel characteristics was possible in the third molar of individual IV:5 and in the teeth of individuals V:2, V:11, V:12, that had recently erupted. In these teeth, enamel was predominantly of normal thickness with some abrasion and chipping of incisal and occlusal surfaces. Enamel was softer than normal and presented a yellowish color with loss of normal translucence. On dental radiographs, the enamel was more radiopaque than dentin, indicating severe hypomineralization.

DNA from 27 individuals of family AMI1 was subjected to a genome-scan with 410 microsatellite markers spaced ~10 cM apart. From the genome-scan data, a maximum two-

point LOD score of 4.6 (θ = 0.00) and multipoint LOD score of 5.1 was obtained at marker D8S373. In order to Fine-map the AI locus, 11 additional markers were genotyped (nine microsatellite and two VNTR markers); nine of these markers were centromeric to D8S373 and two were telomeric. These markers were genotyped in 31 family members. For the genotype data on the additional marker loci and family members, a maximum two-point LOD score of 6.3 was obtained with marker D8S2334 (Table 1) and a maximum multipoint LOD score of 7.5 was obtained with both the LINKMAP and SIMWALK2 programs at marker D8S2334.

Haplotypes were then constructed to determine the critical recombination events (Fig. 1). A recombinant event can be observed in III:8 (Fig. 1), between markers VNTR6 and D8S373, mapping the ADAI locus to a 1.9 cM (2.1 Mb) region between the marker VNTR6 and the telomere. The same interval is also detailed by the three-unit support interval. There are 96 genes in this region reported in the NCBI Entrez Database. Bioinformatics analysis of the hypothetical genes within these 96 identified four that were incorrectly annotated, reducing the number of genes in this region to 92.

Evaluation of genes within candidate interval

Of the 92 genes within the critical interval defined, ten were selected as candidates (*EPPK*, *LOC392275*, *GRINA*, *SLC39A4*, *GPAA1*, *COMMD5*, *VPS28*, *FOXH1*, *ZNF34* and *ZNF517*). Epiplakin (*EPPK*) was selected as it may function as a cytolinker involved in maintaining the integrity of intermediate filament networks in epithelial cells (Jang et al. 2005), and it is present within mucosal epithelial cells (Fujiwara et al. 2001). Similar to sphingomyelin phosphodiesterase 3 (*LOC392275*) was a good candidate as deletion of its related gene, sphingomyelin phosphodiesterase 3 (*Smpd3*), resulted in osteogenesis and dentinogenesis imperfecta in the mouse (Aubin et al. 2005). *GRINA* was chosen as a candidate as it is a subunit of the human NMDA receptor family (Lewis et al. 1996), which function as ligand-gated ion channels for sodium and calcium (Platenik et al. 2000). *SLC39A4* was selected as a candidate as it was a member of the ZIP family of zinc transporters that primarily transport zinc into cells from outside, but can also transport metal ions other than zinc (Dufner-Beattie et al. 2003). *GPAA1* was chosen as it is involved in post-translational glycosylphosphatidylinositol (GPI) anchor attachment that serves as a general mechanism for linking proteins to the cell surface membrane (Ohishi et al. 2000), which could have a role within the extra-cellular amelogenesis process. *COMMD5* was selected as it is a novel calcium-regulated gene coding for a nuclear protein that is potentially involved in the regulation of cell proliferation (Solban et al. 2000) through its participation in a complex that inhibits nuclear factor κB signaling (Burstein et al. 2005). *VPS28* was chosen as it is one of the three target-recognition subunits of the ESCRT-I complex involved in endosomal sorting of ubiquitinated proteins prior to vesicle formation and transport to the cell surface (Raiborg et al. 2003). *FOXH1* encodes a human homolog of Xenopus fork-head activin signal transducer-1 that functions as a transcription factor within the TGF-β signaling pathway by binding to Smad2 and activating an activin response element (ARE) (Zhou et al. 1998). Finally, the two zinc Fingers, *ZNF34* and *ZNF517*, were selected as there is presently nothing known about their expression or function, but their likely role as transcription factors made them good candidates. However, the interrogation of

all exons present within these genes by direct sequencing, with the exception of the highly repetitious 3′ sequence of epiplakin that we were unable to interrogate by this method, failed to identify a causal mutation. Polymorphisms were detected in the exons of some genes, but they failed to segregate with the disease.

Microarray analysis of murine orthologues

To identify additional candidate genes, the expression of the murine orthologues of the genes present in our region, where available, was assessed within the developing mouse tooth during the stages at which amelogenesis takes place, using the Affymetrix mouse genome expression 430 2.0 microarray (MGE430 2.0). The expression pattern of these candidate genes within the developing tooth was compared to that within 16 other mouse tissues to identify those that show differential expression between newborn dental tissue and other tissues. We were specific ally interested in those that exhibited increased expression in dental tissue over other tissues as this could be indicative of a role in amelogenesis.

Of the 92 confirmed genes present within our region, 56 were known genes that had a known orthologue in the mouse (Table 2) that was present on the MGE430 2.0 array. Seven hypothetical genes identified a putative mouse orthologue present on the MGE430 2.0 array, but these were treated with care as their in silico annotation had not been confirmed experimentally. Twenty-nine genes in the candidate region were not present on the MGE430 2.0 array, but of these only four were known genes that had a known murine orthologue, and the remaining 25 were all hypothetical.

Only three of the 56 known genes gave a highly significant *P*-value (Table 2). However, two of these exhibited down-regulation (*CYHR1* & *TIGD5*) in the dental sample, making them poor candidates. The third, *GPAA1*, showed up-regulation, but it had already been sequenced as part of the initial candidate gene mutation screen and no AI-associated mutations had been found within its coding sequence.

Of the nine known genes out of the remaining 53 that had a *P*-value less than 0.05 (Table 2), all but two exhibited down-regulation within the dental tissue, making them poor candidates. The remaining two exhibited slight up-regulation within the dental tissue, but far lower than that of the AI-associated genes (Table 2). LY6H is a glycosylphosphatidylinositol-anchored cell surface glycoprotein that has been reported to be highly expressed in particular subdivisions of the human brain and also in MOLT-3 and −4 acute lymphoblastic leukemia cells, suggesting that it may play a role in both the central nervous system and the immune system (Horie et al. 1998). CPSF1 is one of four members of the Cleavage and Polyadenylation Specificity Factor (CPSF) complex that functions in the 3[H11032] end processing of mRNA precursors (Dantonel et al. 1997). Neither of these was therefore a good candidate for ADAI in this family. All of the putative orthologues of the seven hypothetical genes in our region that were present on the MGE430 2.0 micro-array exhibited down-regulation in the dental sample, also making them poor candidates (data not shown).

Of the four known genes that did not have an orthologue on the microarray, two are poor candidates, *Tmp21-II* and *MAFA*. *Tmp21-II* is a pseudogene copy of the *Tmp21* gene, which is involved in the biosynthetic transport pathway from the endoplasmic reticulum to

the Golgi complex, but it has been reported not to be expressed (Horer et al. 1999) and bioinformatics analysis of its sequence shows it to be disrupted by stop codons (data not shown) making it incapable of producing a functional protein. MAFA is a glucose-regulated and pancreatic beta-cell-specific transcriptional activator for the insulin gene (Kataoka et al. 2002). The remaining two genes were zinc Fingers, *ZNF34* and *ZNF517*, which had already been examined for mutations. There are also the 18 hypothetical genes for which murine orthologues were not identified, but further investigation is required to confirm their annotation and expression before they can be considered as possible candidates.

Discussion

Amelogenesis imperfecta (AI) is a group of genetically and phenotypically diverse forms of defective tooth enamel development. Progress has been made regarding the definition of the genetic basis of AI, but the exact mechanism for the biomineralization process remains largely unknown.

In this study, a novel ADAI locus was mapped to a 2.1 Mb interval on chromosome 8q24.3 region using an extended family. There are 60 known genes in this interval, and 32 hypothetical genes and expressed sequenced tags. Several strong candidate genes in this region included *EPPK*1, *LOC392275*, *GRINA*, *SLC39A4*, *GPAA1*, *COMMD5*, *VPS28*, *FOXH1*, *ZNF34* and *ZNF517*. The gene *LOC392275* seemed like a strong candidate since a deletion of the related *Smpd3* gene in the mouse resulted in osteogenesis and dentinogenesis imperfecta. The exons of each of these genes was sequenced, but no mutation in their coding region was apparent. We did not however, examine the regulatory regions of these genes for a mutation.

Of the five genes implicated in AI to date, amelogenin and enamelin are highly and specific ally expressed in the tooth. Amelogenin is expressed in pre-ameloblasts, ameloblasts and in the epithelial root sheath remnants (Fong and Hammarstrom 2000; Hu et al. 1997; Snead et al. 1988). A low level of amelogenin expression has been recently reported in odontoblasts (Papagerakis et al. 2003). The various isoforms of amelogenin that are involved in the formation of the enamel matrix prior to enamel mineralization represent about 90% of the enamel matrix (Wright et al. 1997). *ENAM* is expressed predominantly by the enamel organ and at a low level in odontoblasts (Hu et al. 2001; Nagano et al. 2003). It is the largest among the least prevalent proteins in the enamel matrix representing about 1–5% of the total protein. *MMP20* is expressed in ameloblasts, pre-ameloblasts, and odontoblasts (Hu et al. 2002), but not in many other tissues surveyed by northern analysis (Llano et al. 1997). *MMP20* encodes a calcium-dependent proteinase that is a member of the matrix metallopeptidase family. It is expressed throughout the secretory stage and during part of the maturation stage. *KLK4* is a calcium-independent serine protease that has a wider pattern of expression than the genes described heretofore. *KLK4* cDNA has been isolated from the brain, prostate, adrenal gland, uterus, spleen, and enamel matrix, and expression has been demonstrated in both ameloblasts and odontoblasts (Hu et al. 2002). Its expression in ameloblasts begins in the transition stage and continues through enamel maturation. *DLX3* is a homeodo-main transcription factor and functional as well as expression studies show that this transcription factor may be instrumental during growth in the control of matrix

deposition and biomineralization in the entire skeleton (Ghoul-Mazgar et al. 2005). Of the genes implicated in AI, *DLX3* is the only gene also implicated in another inherited disorder involving dentition, tricho-dento-osseous syndrome (TDO) (Price et al. 1998). TDO is characterized by kinky or curly hair, dolichocephaly, enamel hypoplasia, increased dental caries, radial dense bones, and occasionally brittle nails.

Based on the expression pattern of AI genes identified to date, we reasoned that candidate genes for AI observed in the family we report here could be identified using microarray analysis of the expression of their murine orthologues within the time period of the developing mouse tooth where amelogenesis occurs. One limitation of this assay was the fact that 29 of the genes in the interval did not identify murine orthologues and thus were not represented on the micro-array, but of these 25 were hypothetical genes that have yet to be experimentally confirmed. Fifty-six of the known genes and seven of the hypothetical genes in our interval identified murine orthologues, with the latter treated as putative, that were present on the Affymetrix Mouse genome expression 430 2.0 micro-array. None of these genes appeared to have expression levels comparable to *AMELX, ENAM, MMP20, KLK4* or *DLX3* in the RNA isolated from the dental tissue (Table 2). Thus, it appears that the mutation in the family we report here is likely in a gene present at lower levels than any of these genes based on these results. Interrogation of their differential expression between the dental and 16 control mouse tissues identified a single candidate for sequence analysis, *GPAA1*, but its sequence had already been interrogated after the initial selection of candidate genes and no causal mutation was identified. We cannot rule out that the causal gene is one of the hypothetical genes that are present within our region but could not be interrogated on the microarray, or that a mutation in the regulatory region of any of these genes could alter their expression leading to a dose-dependent cause for the observed phenotype.

In addition to the novel AI locus we have mapped, there are apparently additional loci associated with autosomal-dominant AI that do not map to any of the Five known AI loci or to the ameloblastin and tuftelin loci implicated by studies in the mouse (Kim et al. 2006). One or more of these could be map to the same region of chromosome 8 and may aid in further refinement of the candidate interval thus, facilitating mutation analysis of candidate genes.

Acknowledgments

This research was supported by grants DE14102 (P.I.P.) and DE06988 (M.L.S.) from the National Institute of Dental and Craniofacial Research. Genotyping services were provided by the Center for Inherited Disease Research (CIDR). CIDR is fully funded through a federal contract from the National Institutes of Health to The Johns Hopkins University, contract number N01-HG-65403. This investigation was conducted in a facility constructed with support from Research Facilities Improvement Program Grant Number C06 (RR10600–01, CA62528–01, RR14514–01) from the National Center for Research Resources, National Institutes of Health.

References

Aldred MJ, Savarirayan R, Crawford PJM (2003) Amelogenesis imperfecta: a classification and catalogue for the 21st century. Oral Dis 9:19–23 [PubMed: 12617253]

Aubin I, Adams CP, Opsahl S, Septier D, Bishop CE, Auge N, Salvayre R, Negre-Salvayre A, Goldberg M, Guenet J-L, Poirier C (2005) A deletion in the gene encoding sphingomyelin

phosphodiesterase 3 (*Smpd3*) results in osteogenesis and dentinogenesis imperfecta in the mouse. Nat Genet 37:803–805 [PubMed: 16025116]

Backman B, Holm AK (1986) Amelogenesis imperfecta: prevalence and incidence in a northern Swedish county. Community Dent Oral Epidemiol 14:43–47 [PubMed: 3456873]

Bartlett JD, Simmer JP, Xue J, Margolis HC, Moreno EC (1996) Molecular cloning and mRNA tissue distribution of a novel matrix metalloproteinase isolated from porcine enamel organ. Gene 183:123–128 [PubMed: 8996096]

Bartlett JD, Skobe Z, Lee DH, Wright JT, Li Y, Kulkarni AB, Gibson CW (2006) A developmental comparison of matrix metalloproteinase-20 and amelogenin null mouse enamel. Eur J Oral Sci 114:18–23 [PubMed: 16674657]

Beniash E, Skobe Z, Bartlett JD (2006) Formation of the dentino enamel interface in enamelysin (*MMP-20*)-deficient mouse incisors. Eur J Oral Sci 114:24–29 [PubMed: 16674658]

Burstein E, Hoberg JE, Wilkinson AS, Rumble JM, Csomos RA, Komarck CM, Maine GN, Wilkinson JC, Mayo MW, Duckett CS (2005) COMMD proteins, a novel family of structural and functional homologs of *MURR1*. J Biol Chem 280:22222–22232 [PubMed: 15799966]

Caterina J, Shi J, Krakora S, Bartlett JD, Engler JA, Kozak CA, Birkedal-Hansen H (1999) Isolation, characterization, and chromosomal location of the mouse enamelysin gene. Genomics 62:308–311 [PubMed: 10610728]

Chosack A, Eidelman E, Wisotski I, Cohen T (1979) Amelogenesis imperfecta among Israeli Jews and the description of a new type of local hypoplastic autosomal recessive amelogenesis imperfecta. Oral Surg Oral Med Oral Pathol 47:148–156 [PubMed: 284277]

Coffield KD, Phillips C, Brady M, Roberts MW, Strauss RP, Wright JT (2005) The psychosocial impact of developmental dental defects in people with hereditary amelogenesis imperfecta. J Am Dent Assoc 136:620–630 [PubMed: 15966649]

Cottingham RWJ, Idury RM, SchaVer AA (1993) Faster sequential genetic linkage computations. Am J Hum Genet 53:252–263 [PubMed: 8317490]

Dantonel J-C, Murthy KGK, Manley JL, Tora L (1997) Transcription factor TFIID recruits factor CPSF for formation of 3′ end of mRNA. Nature 389:399–402 [PubMed: 9311784]

Dong J, Gu TT, Simmons D, MacDougall M (2000) Enamelin maps to human chromosome 4q21 within the autosomal dominant amelogenesis imperfecta locus. Eur J Oral Sci 108:353–358 [PubMed: 11037750]

Dong J, Amor D, Aldred MJ, Gu T, Escamilla M, MacDougall M (2005) *DLX3* mutation associated with autosomal dominant amelogenesis imperfecta with taurodontism. Am J Med Genet Part A 133A:138–141 [PubMed: 15666299]

Dufner-Beattie J, Wang F, Kuo Y-M, Gitschier J, Eide D, Andrews GK (2003) The acrodermatitis enteropathica gene *ZIP4* encodes a tissue-specific, zinc-regulated zinc transporter in mice. J Biol Chem 278:33474–33481 [PubMed: 12801924]

Edgar R, Domrachev M, Lash AE (2002) Gene expression omnibus: NCBI gene expression and hybridization array data repository. Nuc Acids Res 30:207–210

Espiritu-Santo AR, Line SRP (2005) The enamel organic matrix: structure and function. Braz. J Oral Sci 4:716–724

Fong CD, Hammarstrom L (2000) Expression of amelin and amelogenin in epithelial root sheath remnants of fully formed rat molars. Oral Surg Oral Med Oral Pathol Oral Radiol Endod 90:218–223 [PubMed: 10936841]

Fujiwara S, Takeo N, Otani Y, Parry DAD, Kunimatsu M, Lu R, Sasaki M, Matsuo N, Khaleduzzaman M, Yoshioka H (2001) Epiplakin, a novel member of the Plakin family originally identified as a 450-kDa human epidermal autoantigen. Structure and tissue localization. J Biol Chem 276:13340–13347 [PubMed: 11278896]

Gentleman R, Carey V, Bates D, Bolstad B, Dettling M, Dudoit S, Ellis B, Gautier L, Ge Y, Gentry J, Hornik K, Hothorn T, Huber W, Iacus S, Irizarry R, Leisch F, Li C, Maechler M, Rossini A, Sawitzki G, Smith C, Smyth G, Tierney L, Yang J, Zhang J (2004) Bioconductor: open software development for computational biology and bioinformatics. Genome Biol 5:R80 [PubMed: 15461798]

Ghoul-Mazgar S, Hotton D, Lezot F, Blin-Wakkach C, Asselin A, Sautier JM, Berdal A (2005) Expression pattern of *Dlx3* during cell different iation in mineralized tissues. Bone 37:799–809 [PubMed: 16172034]

Hart PS, Hart TC, Michalec MD, Ryu OH, Simmons D, Hong S, Wright JT (2004) Mutation in kallikrein 4 causes autosomal recessive hypomaturation amelogenesis imperfecta. J Med Genet 41:545–549 [PubMed: 15235027]

Hart TC, Hart PS, Gorry MC, Michalec MD, Ryu OH, Uygur C, Ozdemir D, Firatli S, Aren G, Firatli E (2003) Novel *ENAM* mutation responsible for autosomal recessive amelogenesis imperfecta and localised enamel defects. J Med Genet 40:900–906 [PubMed: 14684688]

Horer J, Blum R, Feick P, Nastainczyk W, Schulz I (1999) A comparative study of rat and human Tmp21 (p23) reveals the pseudogene-like features of human *Tmp21-II*. DNA Seq 10:121–126 [PubMed: 10376215]

Horie M, Okutomi K, Taniguchi Y, Ohbuchi Y, Suzuki M, Takahashi E-i (1998) Isolation and characterization of a new member of the human *Ly6* gene family (*LY6H*). Genomics 53:365–368 [PubMed: 9799603]

Hu CC, Fukae M, Uchida T, Qian Q, Zhang CH, Ryu OH, Tanabe T, Yamakoshi Y, Murakami C, Dohi N, Shimizu M, Simmer JP (1997) Cloning and characterization of porcine enamelin mRNAs. J Dent Res 76:1720–1729 [PubMed: 9372788]

Hu JC, Sun X, Zhang C, Liu S, Bartlett JD, Simmer JP (2002) Enamelysin and kallikrein-4 mRNA expression in developing mouse molars. Eur J Oral Sci 110:307–315 [PubMed: 12206593]

Hu JC, Zhang CH, Yang Y, Karrman-Mardh C, Forsman-Semb K, Simmer JP (2001) Cloning and characterization of the mouse and human enamelin genes. J Dent Res 80:898–902 [PubMed: 11379892]

Irizarry RA, Hobbs B, Collin F, Beazer-Barclay YD, Antonellis KJ, Scherf U, Speed TP (2003) Exploration, normalization, and summaries of high density oligonucleotide array probe level data. Biostat 4:249–264

Jang S-I, Kalinin A, Takahashi K, Marekov LN, Steinert PM (2005) Characterization of human epiplakin: RNAi-mediated epiplakin depletion leads to the disruption of keratin and vimentin IF networks. J Cell Sci 118:781–793 [PubMed: 15671067]

Kataoka K, Han S-i, Shioda S, Hirai M, Nishizawa M, Handa H (2002) MafA is a glucose-regulated and pancreatic beta-cell-specific transcriptional activator for the insulin gene. J Biol Chem 277:49903–49910 [PubMed: 12368292]

Kim J-W, Simmer JP, Lin BPL, Seymen F, Bartlett JD, Hu JCC (2006) Mutational analysis of candidate genes in 24 amelo-genesis imperfecta families. Eur J Oral Sci 114:3–12 [PubMed: 16674655]

Kong X, Murphy K, Raj T, He C, White PS, Matise TC (2004) A combined linkage-physical map of the human genome. Am J Hum Genet 75:1143–1148 [PubMed: 15486828]

Lagerstrom M, Dahl N, Nakahori Y, Nakagome Y, Backman B, Landegren U, Pettersson U (1991) A deletion in the amelogenin gene (*AMG*) causes X-linked amelogenesis imperfecta (AIH1). Genomics 10:971–975 [PubMed: 1916828]

Lewis TB, Wood S, Michaelis EK, DuPont BR, Leach RJ (1996) Localization of a gene for a glutamate binding subunit of a NMDA receptor (*GRINA*) to 8q24. Genomics 32:131–133 [PubMed: 8786101]

Llano E, Pendas AM, Knauper V, Sorsa T, Salo T, Salido E, Murphy G, Simmer JP, Bartlett JD, Lopez-Otin C (1997) Identification and structural and functional characterization of human enamelysin (*MMP-20*). Biochemistry 36:15101–15108 [PubMed: 9398237]

Luo W, Wen X, Wang HJ, MacDougall M, Snead ML, Paine ML (2004) In vivo overexpression of Tuftelin in the enamel organic matrix. Cells Tiss Organs 177:212–220

Nagano T, Oida S, Ando H, Gomi K, Arai T, Fukae M (2003) Relative levels of mRNA encoding enamel proteins in enamel organ epithelia and odontoblasts. J Dent Res 82:982–986 [PubMed: 14630899]

O'Connell JR, Weeks DE (1998) PedCheck: a program for identification of genotype incompatibilities in linkage analysis. Am J Hum Genet 63:259–266 [PubMed: 9634505]

Ohishi K, Inoue N, Maeda Y, Takeda J, Riezman H, Kinoshita T (2000) Gaa1p and Gpi8p are components of a glycosylphosphatidylinositol (GPI) transamidase that mediates attachment of GPI to proteins. Mol Biol Cell 11:1523–1533 [PubMed: 10793132]

Ozdemir D, Hart PS, Ryu OH, Choi SJ, Ozdemir-Karatas M, Firatli E, Piesco N, Hart TC (2005) MMP20 active-site muta tion in hypomaturation amelogenesis imperfecta. J Dent Res 84:1031–1035 [PubMed: 16246936]

Paine ML, Wang H-J, Luo W, Krebsbach PH, Snead ML (2003) A Transgenic animal model resembling amelogenesis imperfecta related to ameloblastin overexpression. J Biol Chem 278:19447–19452 [PubMed: 12657627]

Paine ML, White SN, Luo W, Fong H, Sarikaya M, Snead ML (2001) Regulated gene expression dictates enamel structure and tooth function. Mat Biol 20:273–292

Papagerakis P, MacDougall M, Hotton D, Bailleul-Forestier I, Oboeuf M, Berdal A (2003) Expression of amelogenin in odontoblasts. Bone 32:228–240 [PubMed: 12667550]

Platenik J, Kuramoto N, Yoneda Y (2000) Molecular mechanisms associated with long-term consolidation of the NMDA signals. Life Sci 67:335–364 [PubMed: 11003045]

Price JA, Bowden DW, Wright JT, Pettenati MJ, Hart TC (1998) Identification of a mutation in *DLX3* associated with trichodento-osseous (TDO) syndrome. Hum Molec Genet 7:563–569 [PubMed: 9467018]

Price JA, Wright JT, Walker SJ, Crawford PJM, Aldred MJ, Hart TC (1999) Tricho-dento-osseous syndrome and amelogenesis imperfecta with taurodontism are genetically distinct conditions. Clin Genet 56:35–40 [PubMed: 10466415]

Raiborg C, Rusten TE, Stenmark H (2003) Protein sorting into multivesicular endosomes. Curr Opin Cell Biol 15:446–455 [PubMed: 12892785]

Rajpar MH, Harley K, Laing C, Davies RM, Dixon MJ (2001) Mutation of the gene encoding the enamel-specific protein, enamelin, causes autosomal-dominant amelogenesis imperfecta. Hum Mol Genet 10:1673–1677 [PubMed: 11487571]

Schuler GD (1997) Sequence Mapping by Electronic PCR. Genome Res 7:541–550 [PubMed: 9149949]

Smyth GK (2004) Linear models and empirical bayes methods for assessing differential expression in microarray experiments. Stat Appl Genet Mol Biol 3:Article 3

Snead ML, Luo W, Lau EC, Slavkin HC (1988) Spatial- and temporal-restricted pattern for amelogenin gene expression during mouse molar tooth organogenesis. Development 104:77–85 [PubMed: 3253061]

Sobel E, Lange K (1996) Descent graphs in pedigree analysis: applications to haplotyping, location scores, and marker-sharing statistics. Am J Hum Genet 58:1323–1337 [PubMed: 8651310]

Solban N, Jia H-P, Richard S, Tremblay S, Devlin AM, Peng J, Gossard F, Guo D-F, Morel G, Hamet P, Lewanczuk R, Tremblay J (2000) *HCaRG*, a novel calcium-regulated gene coding for a nuclear protein, is potentially involved in the regulation of cell proliferation. J Biol Chem 275:32234–32243 [PubMed: 10918053]

Stephanopoulos G, Garefalaki ME, Lyroudia K (2005) Genes and related proteins involved in amelogenesis imperfecta. J Dent Res 84:1117–1126 [PubMed: 16304440]

Sundell S (1986) Hereditary amelogenesis imperfecta. An epidemiological, genetic and clinical study in a Swedish child population. Swed Dent J Suppl 31:1–38 [PubMed: 3460191]

Witkop CJ (1976) Clinical aspects of dental anomalies. Int Dent J 26:378–390 [PubMed: 186412]

Wright JT, Daly B, Simmons D, Hong S, Hart SP, Hart TC, Atsawasuwan P, Yamauchi M (2006) Human enamel phenotype associated with amelogenesis imperfecta and a kallikrein-4 (g.2142G > A) proteinase mutation. Eur J Oral Sci 114:13–17 [PubMed: 16674656]

Wright JT, Hall K, Yamauchi M (1997) The protein composition of normal and developmentally defective enamel. Ciba Found Symp 205:85–99 [PubMed: 9189619]

Zhou S, Zawel L, Lengauer C, Kinzler KW, Vogelstein B (1998) Characterization of Human FAST-1, a TGF[beta] and Activin Signal Transducer. Mol Cell 2:121–127 [PubMed: 9702198]

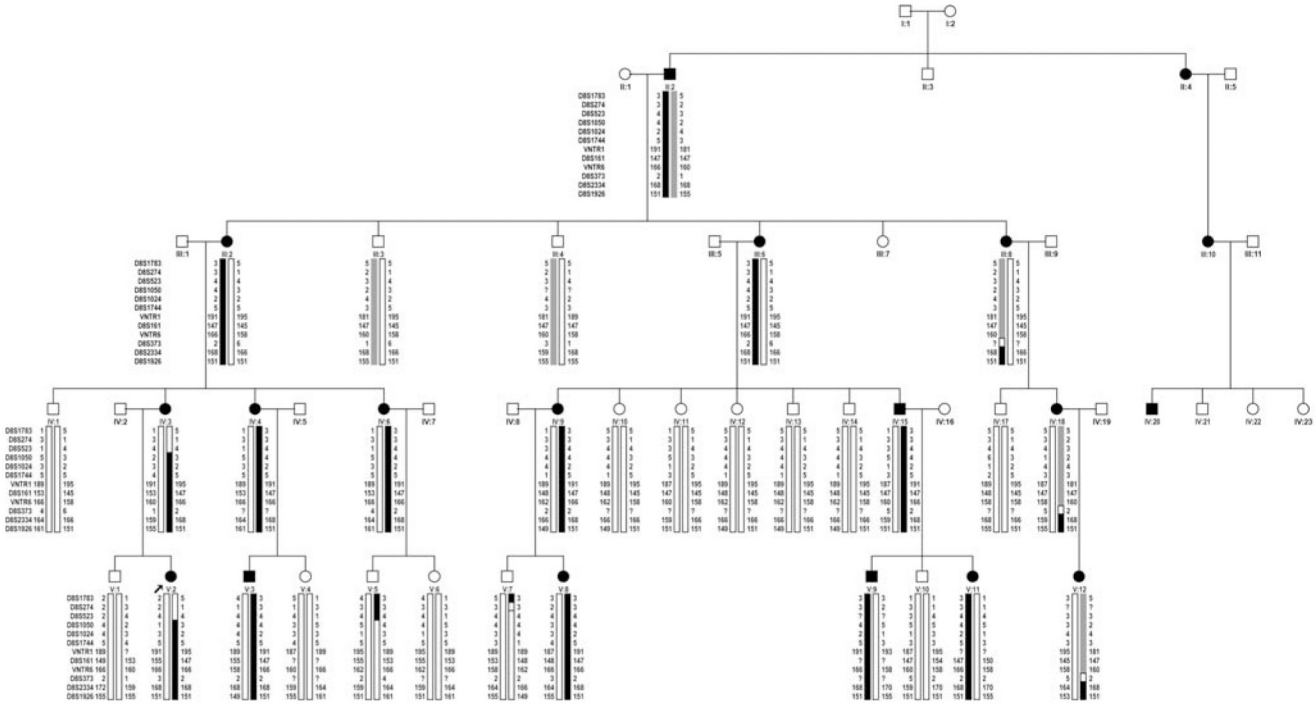

Fig. 1.

Pedigree of family AMI1 segregating autosomal dominant hypomineralized amelogenesis imperfecta. Affected males and females are indicated by *filled squares* and *circles*, respectively. The proband is marked by the *arrow*. The genotypes of the microsatellite markers that were used to define the candidate interval are shown below each individual used in the linkage analysis screen. The *black bar* represents the marker haplotype that tracks with the affected status, and the *grey bar* indicates the marker haplotype that tracks with the unaffected status. *White bars* indicate marker haplotypes acquired from individuals who married into family AMI1

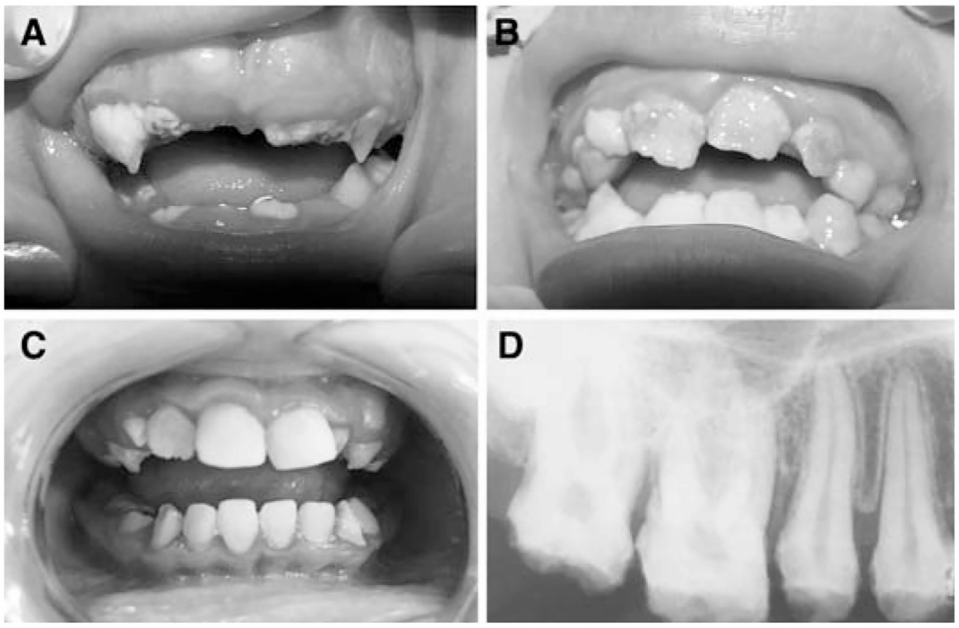

Fig. 2.

Oral photographs of **a** individual V:11, **b** individual V:8, and **c** individual V:2 from family AMI1. **d** A dental Xray of the molars and premolars of individual V:2

Table 1

Two-point LOD scores used in the Fine-mapping of the locus associated with autosomal dominant AI in family AMI1

Marker	Genetic position[a]	Physical position[b]	0								
			0	**0.01**	**0.02**	**0.03**	**0.04**	**0.05**	**0.1**	**0.2**	**0.3**
D8S1783	154.71	137,339,899	−0.58	0.92	1.46	1.75	1.95	2.08	2.36	2.21	1.68
D8S274	155.94	137,687,609	−4.66	0.61	1.14	1.42	1.6	1.73	1.97	1.81	1.34
D8S523	156.5	138,217,023	−2.47	0.09	0.37	0.53	0.64	0.72	0.9	0.89	0.69
D8S1050	160.14	139,724,989	−3.35	2.26	2.77	3.03	3.18	3.28	3.39	2.95	2.18
D8S1024	165.78	141,497,876	−0.86	1.62	1.86	1.98	2.04	2.08	2.06	1.7	1.19
D8S1744	168.86	143,101,135	−1.36	0.76	1.02	1.15	1.24	1.29	1.37	1.2	0.87
VNTRI	169.09	143,214,611	1.54	4.24	4.44	4.51	4.54	4.53	4.31	3.5	2.48
D8S161	169.57	143,444,873	5.07	4.99	4.92	4.84	4.76	4.68	4.27	3.39	2.4
VNTR6	170.69	143,988,705	1.36	4.04	4.25	4.33	4.36	4.36	4.17	3.42	2.45
D8S373	**171.32**	**144,296,507**	**4.58**	**4.5**	**4.43**	**4.36**	**4.29**	**4.21**	**3.83**	**3**	**2.06**
D8S2334	*171.32*	*146,101,309*	*6.27*	*6.18*	*6.08*	*5.99*	*5.89*	*5.79*	*5.29*	*4.2*	*2.98*
D8S1926	172.62	146,114,938	2.82	2.77	2.72	2.67	2.62	2.57	2.31	1.77	1.17

The marker name shown in bold was present within the genome-wide linkage panel. A maximum two-point LOD score of 6.3 and a maximum multipoint LOD score of 7.5 were obtained at marker D8S2334 (highlighted in italics)

[a] Sex-averaged Kosambi map distance (cM) from the Rutgers map (Kong et al. 2004)

[b] Sequence-based physical map distance in bases according to Build 35 of the human reference sequence (International Human Genome Sequence Consortium 2004)

Table 2

Differential expression data for the mouse orthologues of the Five genes (*Amelx, Enam, Mmp20, Klk4*, and *Dlx3*), mutations within which are known to cause AI, and 56 human genes from the ADAI candidate region that have a known orthologue in mouse

Gene ID	Gene name	Log_2 (Diff.)	*P* value	LOD score
AMELX	Amelogenin X chromosome	7.603	5.15×10^{-20}	40.663
ENAM	Enamelin	7.435	4.57×10^{-18}	37.317
KLK4	Kallikrein	5.293	9.37×10^{-17}	34.780
DLX3	Distal-less homeobox 3	3.388	3.44×10^{-10}	19.587
CYP11B2	Cytochrome P450, family 11, subfamily b, member 2	−0.346	0.131	−4.824
LY6E	Lymphocyte antigen 6 complex, locus E	−0.973	**0.030**	−2.823
LY6H	Lymphocyte antigen 6 complex, locus H	1.836	**0.040**	−3.239
LOC338328	High density lipoprotein-binding protein	−0.332	0.754	−7.093
ZFP41	Zinc finger protein 41 homolog (mouse)	−0.192	0.060	−5.373
GL14	GLI-kruppel family member GL14	−0.375	0.310	−5.991
TOP1MT	Topoisomerase (DNA) I, mitochondrial	−0.439	0.411	−6.366
RHPN1	Rhophilin, Rho GTPase binding protein 1	−0.163	0.747	−7.084
ZC3HDC3	Zinc finger CCCH type domain containing 3	0.246	0.224	−5.552
GSDMDC1	Gasedermin domain containing 1	0.163	0.524	−6.674
NAPRT1	Nicotinate phosphoribosyltransferase domain containing 1	−1.042	**0.034**	−4.856
EEF1D	Eukaryotic translation elongation factor 1 delta	−0.109	0.743	−7.078
TIGD5	Tigger transposable element derived 5	0.674	$\mathbf{1.15 \times 10^{-4}}$	4.314
PYCRL	Pyrroline-5-carboxylate reductase-like	−0.066	0.883	−7.220
TSTA3	Tissue specific transplantation antigen P35B	−0.350	0.519	−6.662
ZNF623	Zinc finger protein 623	−0.056	0.794	−7.226
ZNF707	Zinc finger protein 707	0.065	0.798	−7.227
ERK8	Extracellular singal-regulated kinase 8	0.060	0.853	−7.198
FLJ46072	FLJ46072 protein	0.810	0.336	−6.097
SCRIB	Scribbled homolog *(Drosophila)*	0.074	0.897	−7.229
SIAHBP1	Fuse-binding protein-interacting repressor	−0.151	0.650	−6.934
NRBP2	Nuclear receptor binding protein 2	0.569	0.366	−6.824
EPPK1	*Epiplakin 1*	*0.171*	*0.876*	*−7.215*

Gene ID	Gene name	Log_2 (Diff.)	*P* value	LOD score
PLEC1	Plectin 1, intermediate filament binding protein 500 kDa	−2.099	**0.002**	0.816
GRINA	*Glutamate receptor, ionotropic, N-methyl D-asparate-associated protein 1*	*−1.571*	***0.009***	*−1.210*
SPATC1	Spermatogensesis and centirole associated 1	0.124	0.821	−7.235
OPLAH	5-oxoprolinase(ATP-hydrolysing)	0.657	**0.002**	0.460
EXOSC4	Exosome component 4	−0.250	0.328	−6.065
GPAA1	*GPAA1P anchor attachment protein 1 homolog (yeast)*	*1.234*	$\boldsymbol{3.35 \times 10^{5}}$	*5.808*
CYC1	Cytochrome c-1	−0.775	0.084	−4.220
SHARPIN	Shank-interacting protein-like 1 alpha	−0.436	0.092	−4.348
MAF1	Homolog of yeast MAF 1	−0.404	0.376	−6.246
BOP1	Block of proliferation 1	−0.472	0.210	−5.463
HSF1	Heat shock transcription factor 1	−0.396	0.307	−5.977
DGAT1	Diacylglycercol O-acyltransferase homolog 1 (mouse)	−0.574	0.349	−6.149
SCRT1	Scratch homolog 1, zinc finger protein *(Drosophila)*	−0.330	0.539	−6.711
FBXL6	F-box and leucine-rich repeat protein 6	−0.100	0.840	−7.188
GPR172A	G protein-coupled receptor 172A	0.362	0.223	−5.542
ADCK5	aarF domain containing kinase 5	−0.699	0.123	−4.731
CPSF1	Cleavage and polyadenylation specific factor 1, 160 kDa	−0.740	**0.004**	−0.148
SLC39A4	*Solute carrier family 39 (zinc transporter), member 4*	*-0.186*	*0.889*	
VPS28	*Vacuolar protein sorting 28 (yeast)*	*−0.455*	*0.057*	
NFKBIL2	Nuclear factor of kappa light polypeptide gene enhancer in B-cells inhibitor-like 2	−0.197	0.680	−6.985
CYHR1	Cysteine and histidine rich 1	0.980	$\boldsymbol{3.06 \times 10^{-4}}$	3.081
KIFC2	Kinesin family member c2	0.242	0.374	−6.242
FOXH1	*Forkhead box H1*	*0.849*	***0.001***	*−1.658*
PPP1R16A	Protein phosphatase 1, regulatory (inhibitor) subunit 16A	−0.356	0.243	−5.657
GPT	Glutamuic-pyruvate transaminase (alanine aminotransferase)	−0.753	**0.012**	−1.566
MFSD3	Major facilitator superfamily domain containing 3	−0.278	0.364	−6.820
RECQL4	RecQ protein-like 4	−0.183	0.673	−6.974
LRRC14	Leucine rich repeat containing 14	0.516	0.094	−4.380
LRRC24	Leucine rich repeat containing 24	−0.310	0.453	−6.960
ZNF251	Zinc finger protein 251	0.373	0.279	−5.848
RPL8	Ribosomal protein L8	−0.165	0.714	−7.037

Hum Genet. Author manuscript; available in PMC 2018 October 08.

Gene ID	Gene name	Log_2 (Diff.)	*P* value	LOD score
ZNF7	Zinc Wnger protein 7 (KOX 4, clone HF.16)	−0.582	0.387	−6.287
COMMD5	*COMM domain containing 5*	*−0.439*	***0.020***	*−2.288*
ZNF647	Zinc Wnger protein 647	0.342	0.453	−6.487
ZNF16	Zinc Wnger protein 16 (KOX 9)	−0.375	0.310	−5.991

Seven hypothetical genes identified a putative mouse orthologue present on the MGE 430 2.0 array, but were omitted from this table. Of the 29 genes not present on the MGE 430 2.0 array, only four have a known murine orthologue, the remaining 25 are all hypothetical. Log-odds of differential expression were calculated by empirical Bayes shrinkage of the gene-wise sample variances towards a common value (Smyth 2004)

P-values less than 0.05 are highlighted in bold

Seven of the ten genes that were sequenced and present on the MGE430 2.0 microarray are highlighted in italics